Quantum magnetotransport properties of short quantum wires

Tae-ik Park and Godfrey Gumbs*
Department of Physics and Astronomy, Hunter College of the City University of New York, 695 Park Avenue, New York, New York 10021

M. Pepper†
Cavendish Laboratory, University of Cambridge, Madingley Road, Cambridge CB3 0HE, United Kingdom
(Received 28 March 1997)

The longitudinal and transverse quantum magnetotransport coefficients of a two-dimensional electron gas in a perpendicular magnetic field for short quantum wires are calculated in the low-magnetic-field region ($B \lesssim 0.3$ T) using the Kubo method. The quantum wire channel is simulated by controlling the steepness and strength of the potential barrier. The calculated results have steplike features in the transverse conductivities as the Fermi energy crosses a Landau level for weak modulation potentials and giant low-field peaks in the transverse resistivities when the potential is strong. In addition, the Hall resistivity is quenched in the low-magnetic-field region. An interesting feature is the negative Hall resistivity which arises from backscattering off the edges of confinement for short quantum wires. [S0163-1829(97)03735-1]

I. INTRODUCTION

Following the success in understanding the physics and the device applications of two-dimensional (2D) heterostructures, the natural trend has been to reduce their dimensionality by modulation techniques to one-dimensional (1D) systems called quantum wires (QW's) or antiwires. For ideal QW's, the low-field conductance was shown to be quantized with the conductance equal to e^2/h times the number of channels occupied.[1] However, in a realistic QW, there are some aspects which deviate from the ideal. One of these is that the QW realized in a quantum point contact is not infinitely long and does not have perfect translational symmetry. This kind of deviation gives rise to different regimes of conductance.[2] The regimes depend on the length scales of the sample, i.e., the length L, width W of the QW or constriction and the elastic mean free path l. When $L > W \gg l$, electrons are localized longitudinally and transversely on the length scale l. So, in this case, the wire modes no longer have meaning. In other words, the electrons no longer see the one dimensionality of the wire. Therefore, no states exist that extend from one end of the wire to the other. This regime is similar to the weakly localized 2D modulation case. However, if $l \gg L$ and W, the situation becomes different. In this case, the electrons are affected by the boundaries of the wire and quantum states exist that extend from one end of the wire to the other. These occupied quantum channels carry the current along the wire. The conductance is then determined by the quantum mechanical transmission probability of different states between the two ends, due to the chemical potential difference. If the width W of the QW is small compared with the Fermi wavelength or the cyclotron radius when the magnetic field is applied perpendicular to the 2D sheet, then there is quantum ballistic transport. Ballistic transport in QW's has properties which cannot be accounted for classically, since the electrons are wavelike in nature. This means that the wires act as waveguides for the electrons so that the resistance of a wire loses its local meaning. In this regime, the boundary conditions on the contacts become very important and a system of connected wires show a nonlocal behavior. Therefore, a current flowing between two contacts might influence the voltage between two other contacts, even though classically no current should flow between the two voltage probes. Accordingly, this regime strongly depends on the sample geometry. One of these is the well-known quenching in the Hall regime at low magnetic fields. Traditionally, this quenching has been explained by the collimation of the electrons. In this case, the ratio of the longitudinal momentum to the transverse momentum increases and, near zero magnetic field, these collimated electrons are preferentially transmitted straight through the junction, and the Hall voltage is quenched.[3]

Another Hall effect in the ballistic wire is the negative Hall resistivity. This resistivity in ballistic wire transport has been dealt with both experimentally and theoretically.[3–9] These papers show that the negative Hall resistivity depends on the sample geometry. In narrow ballistic wires with high mobility, the predominant source of scattering is the reflection of the carriers off the confining potential. So, by changing the geometry of the intersection of the Hall probes, they showed quenched, enhanced, and even negative Hall resistances at low magnetic fields. Also Buttiker showed theoretically that the negative Hall resistance was a signature of four-terminal resistance measurements.[7] Another example of the negative Hall resistance has been shown in the four terminal magnetoresistance of a multichannel electron waveguide by Timp *et al.*[10] In Ref. 10, submicrometer wires were fabricated in extremely high mobility $GaAs/Al_xGa_{1-x}As$ heterostructures and only a few transverse, one-dimensional subbands or channels carry the current because the width of the QW is comparable to an electron wavelength. In this wire, the negative Hall resistances through the Hall probe at different locations are observed. All of these depend on the geometry of the sample or measuring probe. In addition to this, the length and termination of a piece of wire not connected to a contact will change the behavior of the rest of the

structure.[1] The length L, the width W of the wire, and the height of the potential barrier are all crucial factors in ballistic Hall resistances. To the best of our knowledge, there has so far not been a detailed theoretical study of the ballistic Hall effect due to the length or termination of a piece of wire. So, in this paper, we calculate theoretically the negative Hall resistance due to the termination of a piece of QW, i.e., we carry out calculations for short QW's.

II. THEORETICAL FORMULATION OF THE PROBLEM

The single-particle Hamiltonian for a 1D array of QW's in a two-dimensional electron gas (2DEG) located in the x-y plane with a uniform perpendicular magnetic field $\mathbf{B}=B\hat{z}$ along the z axis is given by

$$\mathcal{H}_0=\frac{1}{2m^*}[-i\hbar\nabla+e\mathbf{A}(\mathbf{r})]^2+U_L(\mathbf{r}), \tag{1}$$

where m^* is the effective mass of an electron with charge $-e$, $\mathbf{r}$ is a 2D vector in the x-y plane, and $\mathbf{A}(\mathbf{r})=(0,Bx,0)$ is the vector potential in the Landau gauge. The lattice potential $U_L(\mathbf{r})$ in Eq. (1) represents the effect due to modulation which we take as

$$U_L(\mathbf{x})=V_0\left[\cos\left(\frac{2\pi x}{a}\right)\right]^{2N}, \tag{2}$$

for modulation in the x direction. When the modulation is in the y direction, we make the replacement $x\rightarrow y$ in Eq. (2) to obtain the potential. In this notation, $V_0>0$ denotes the height of the potential barrier, and a is the period of the potential. The value of N represents the steepness of the slope of the potential. As N is increased, the region between adjacent potential barriers gets wider. If V_0 is large, an electron may be trapped within a channel and the model represents a parallel array of QW's. The reason for taking $2N$ as the power in Eq. (2) is to make sure that the potential is positive when $V_0>0$.

We use the Kubo formalism for the static local conductivity which is given by

$$\sigma_{\mu\nu}=i\hbar e^2\int dE\ f_0(E)\ \mathrm{Tr}\left[\hat{\mathbf{v}}_{\mathrm{op}}\frac{dG_E^+}{dE}\hat{\mathbf{v}}_{\mathrm{op}}\delta(E-\mathcal{H}_0)-\hat{\mathbf{v}}_{\mathrm{op}}\delta(E-\mathcal{H}_0)\hat{\mathbf{v}}_{\mathrm{op}}\frac{dG_E^-}{dE}\right], \tag{3}$$

where $f_0(E)$ is the Fermi-Dirac distribution function, $\hat{\mathbf{v}}_{\mathrm{op}}$ is the velocity operator, and $G_E^{\pm}$ are the retarded and advanced Green's functions.

The single-particle eigenfunctions for the Hamiltonian in Eq. (1) are given by

$$\psi_{j,X_0}(\mathbf{r})=\sum_n C_n(j,X_0)\,\phi^{(0)}_{n,X_0}(\mathbf{r}), \tag{4}$$

where

$$\phi^{(0)}_{n,X_0}(\mathbf{r})=\frac{\exp[-i(X_0)y/l_H^2]}{\sqrt{L_y}}\sqrt{\frac{1}{\pi^{1/2}l_H 2^n n!}}\times\exp[-(x-X_0)^2/2l_H^2]H_n\left(\frac{x-X_0}{l_H}\right). \tag{5}$$

In Eqs. (4) and (5), $n=0,1,2,\ldots$ is a Landau level index and $H_n(x)$ is the nth order Hermite polynomial. Also, $L_y=N_y a$ is the sample length, in the y direction, $X_0=k_y l_H^2$ is the guiding center, $l_H=\sqrt{\hbar/eB}$ is the magnetic length, and k_y is a wave vector along the y direction. The expansion coefficients $C_n(j,X_0)$ in Eq. (4) are determined from the following matrix equation:

$$\sum_n\left[[E_n^{(0)}-E_j(X_0)]\delta_{n,n'}+\frac{V_0}{a^2 l_H\pi^{1/2}}\sqrt{\frac{1}{2^{n+n'}n!n'!}}\times B_{n,n'}(X_0)\right]C_n(j,X_0)=0, \tag{6}$$

as well as the orthonormality condition:

$$\sum_n C_n^*(j,X_0)C_n(j',X_0')=\delta_{j,j'}\delta_{X_0,X_0'}.$$

From this calculation, we also obtain the secular equation which determines the energy eigenvalues $E_j(X_0)$:

$$\mathrm{Det}\left[[E_n^{(0)}-E_j(X_0)]\delta_{n,n'}+\frac{V_0}{a^2 l_H\pi^{1/2}}\sqrt{\frac{1}{2^{n+n'}n!n'!}}B_{n,n'}(X_0)\right]=0. \tag{7}$$

Here, $E_n^{(0)}=(n+1/2)\hbar\omega_c$ is the energy for the nth Landau level with eigenfunction $\phi_n^{(0)}(\mathbf{r})$ for a homogeneous 2DEG and the matrix element $B_{n,n'}(X_0)$ appearing in Eqs. (6) and (7) is defined as follows, for the potential in Eq. (2):

$$\begin{aligned}8B_{n,n'}(X_0)&\equiv\langle\phi^{2\ (0)}_{n',X_0}(\mathbf{r})|U_L(\mathbf{x})|\phi^{2\ (0)}_{n,X_0}(\mathbf{r})\rangle\\&=\int_{-\infty}^{\infty}dx\ \exp\left[-\frac{(x-X_0)^2}{l_H^2}\right]H_n\left(\frac{x-X_0}{l_H}\right)\times H_{n'}\left(\frac{x-X_0}{l_H}\right)\cos^{2N}(2\pi x/a).\end{aligned} \tag{8}$$

III. NUMERICAL RESULTS AND DISCUSSION

We now present numerical results for the band parts of the longitudinal and transverse quantum magnetotransport coefficients when the 2DEG is modulated in the x direction and compare these results with those obtained when the modulation is in the y direction. We also vary the lengths of the wires to study the dependence of the magnetotransport coefficients on the wire length.

A. Transverse conductivity

In Figs. 1(a)–1(c), we present numerical results at $T=0$ K for the transverse conductivity σ_{xx}, i.e., the current and the applied electric field are along the x direction which is at right angles to the channels produced by the modulation po-

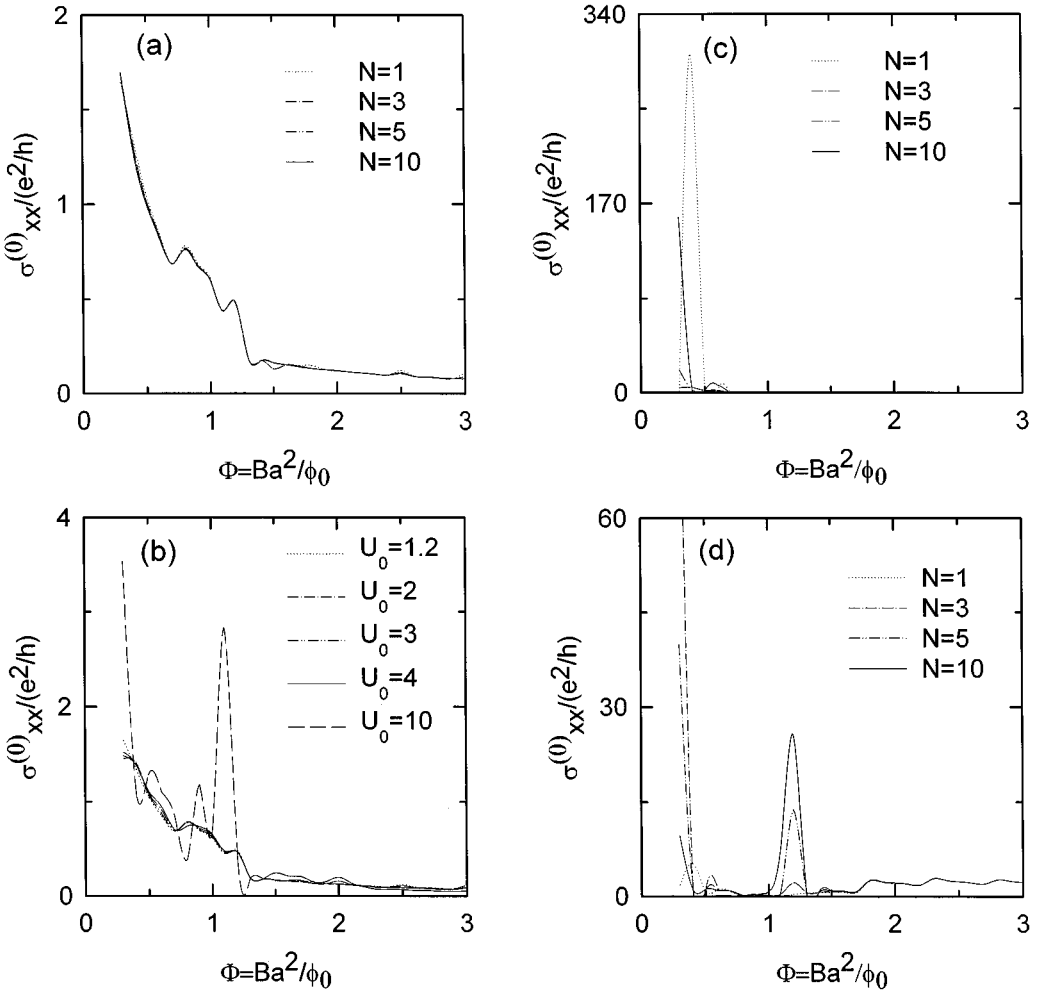

FIG. 1. The computed conductivity σ_{xx} as a function of the magnetic flux for the potential in Eq. (2) for (a) four values of N and $U_0=1.2$; (b) $N=1$ and five different values of the potential strength U_0; (c) $U_0=100.0$ is fixed and N takes the values 1, 3, 5, 10; (d) same as (a) except that $U_0=100.0$ and the modulation is along the y direction. The electron density is given by $n_{2D}a^2=0.5$ and $L_x=L_y=80$ Å.

tential in Eq. (2), for several potential barrier heights and steepness of their slopes. The plots are presented as a function of the flux through a unit cell $\Phi=Ba^2/\phi_0$, in units of the flux quantum $\phi_0=h/e$. In Fig. 1(a) where the modulation is weak with $V_0=0.156$ meV, there are steps in σ_{xx} at low magnetic fields. These arise when the Fermi level crosses a Landau level (LL). For the parameters chosen in our calculation, the Fermi level is in the $n=3$ LL up to $\Phi=0.7$, then it is in $n=1$ up to $\Phi=1.2$, and $n=0$ up to $\Phi=3.0$. This feature in the electrical conductivity has been observed in other related calculations.[11] Furthermore, as Fig. 1(a) shows, σ_{xx} is not appreciably affected when the width of the potential barrier is changed with N. This is understood by noting that at $T=0$ K, the contribution to σ_{xx} comes only from electrons near the Fermi level. Defining the dimensionless potential variable by $U_0=m^*a^2V_0/\sqrt{2}\pi\hbar^2$, we have $V_0=0.156$ meV for $U_0=1.2$, $a=200$ nm, and $m^*=0.067m_e$, where m_e is the free electron mass. All Fermi energies in the whole range of Φ shown in the figures are comparable with or lie above the top of the potential, i.e., $E_F>V_0=0.156$ meV. Subsequently, electrons with eigenenergies above the Fermi level are not affected by the variation of the width of the potential barrier with N, leading to the negligible changes in the results presented in Fig. 1(a). These conclusions are supported by our results in Figs. 1(b) and 1(c). In these figures, we see how the σ_{xx} is modified as the strength of the potential U_0 is varied. In Fig. 1(d), we show how σ_{xx} is affected by changing the value of N in the potential for modulation in the y direction instead of the x direction as in Fig. 1(a). The conductivity is larger in Fig. 1(d) since the applied electric field and the current are along the direction of the channel.

In Fig. 1(b), we chose $U_0=1.2$, 2.0, 3.0, 4.0, 10.0, which correspond to $V_0=0.156$, 0.253, 0.380, 0.506, and 1.265 meV, respectively, for $a=200$ nm. The Fermi energies satisfy $0.190<E_F<0.443$ for $0.3<\Phi<0.7$; $0.217<E_F<0.322$ for $0.8<\Phi<1.2$; $0.116<E_F<0.152$ for $1.3<\Phi<1.7$; $0.161<E_F<0.197$ for $1.8<\Phi<2.2$; $0.206<E_F<0.241$ for $2.3<\Phi<2.7$, and $0.250<E_F<0.268$ for $0.8<\Phi<3.0$, respectively, where the Fermi energy is in meV. The value of $V_0=1.265$ meV, which corresponds to $U_0=10$, is well above the Fermi levels. The steplike features are maintained from $U_0=1.2$ up to $U_0=4.0$ but not for $U_0=10$. When $U_0=10$, the steplike features in σ_{xx} are modified and there are some peaks due to the resonant backscattering off the potential barrier. These peaks do not appear in Fig. 1(c)

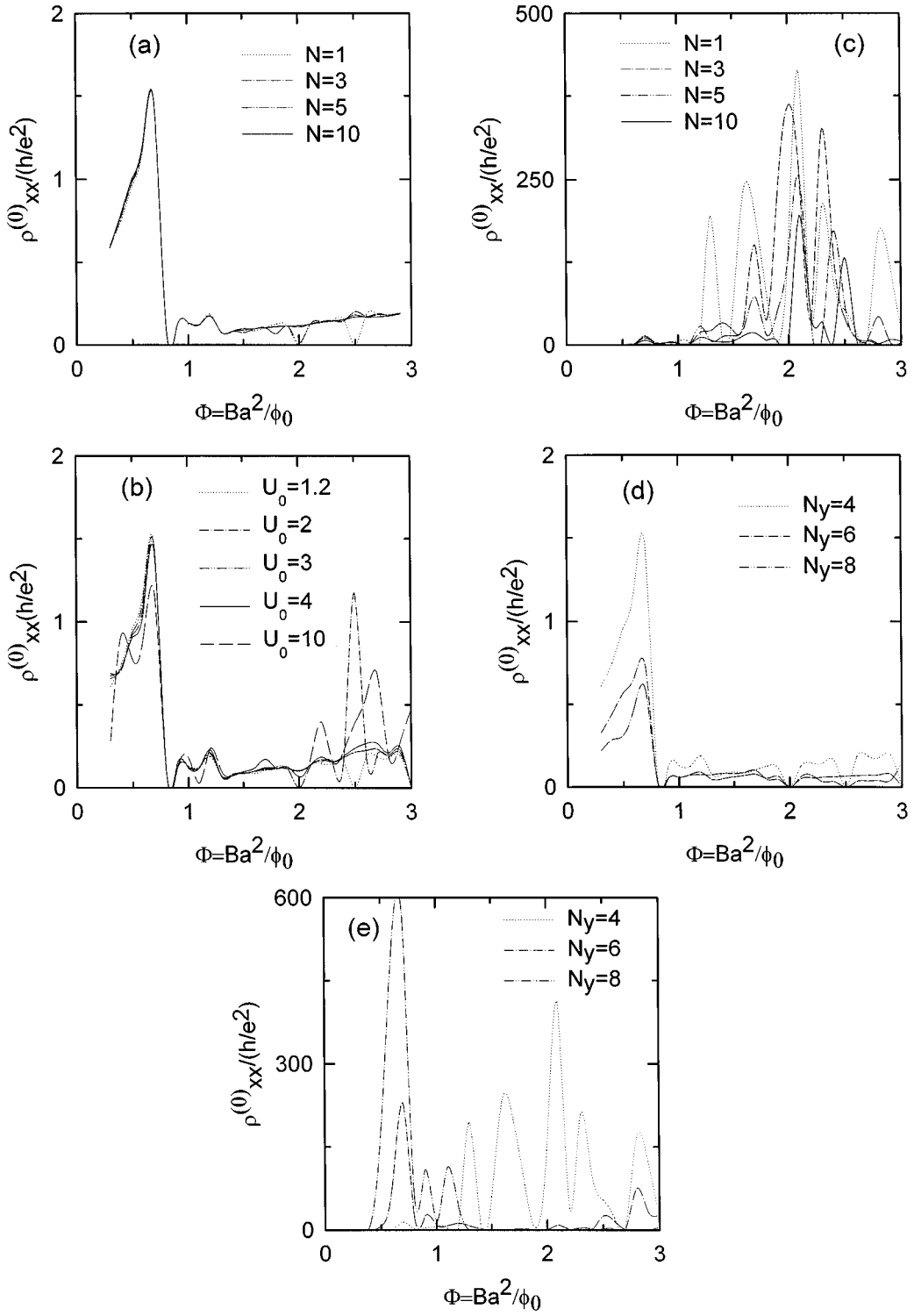

FIG. 2. Plots of ρ_{xx} as a function of the magnetic flux for the potential in Eq. (2) for (a) four values of N and $U_0=1.2$; (b) $N=1$ and five different values of the potential strength U_0; (c) $U_0=100.0$ is fixed and N takes the values 1, 3, 5, 10; (d) $U_0=1.2$, $N=1$ for three wire lengths $L_y=N_y a$ and $a=200$ nm; (e) same as (d) except that $U_0=100.0$. The electron density is given by $n_{2D}a^2=0.5$ and the sample length in the x direction is $L_x=N_x a$, where $N_x=4$.

when $U_0=100$ which means that the effect produced when the Fermi level crosses a LL is reduced in the strong modulation regime. However, as Fig. 1(d) shows, there are peaks in σ_{xx} even when the modulation is strong, if the current and the external electric field are along the channel, i.e., when the modulation is in the y direction. The large conductivities due to the open orbits are generated in the low magnetic field regime and there is another peak around $\Phi=1.2$. This peak is due to the resonant scattering with the potential barrier since it strongly depends on the width of the potential barrier. For this calculation, the cyclotron orbit for a flux of $\Phi i \cong 1.2$ is about the channel width. When N increases, the

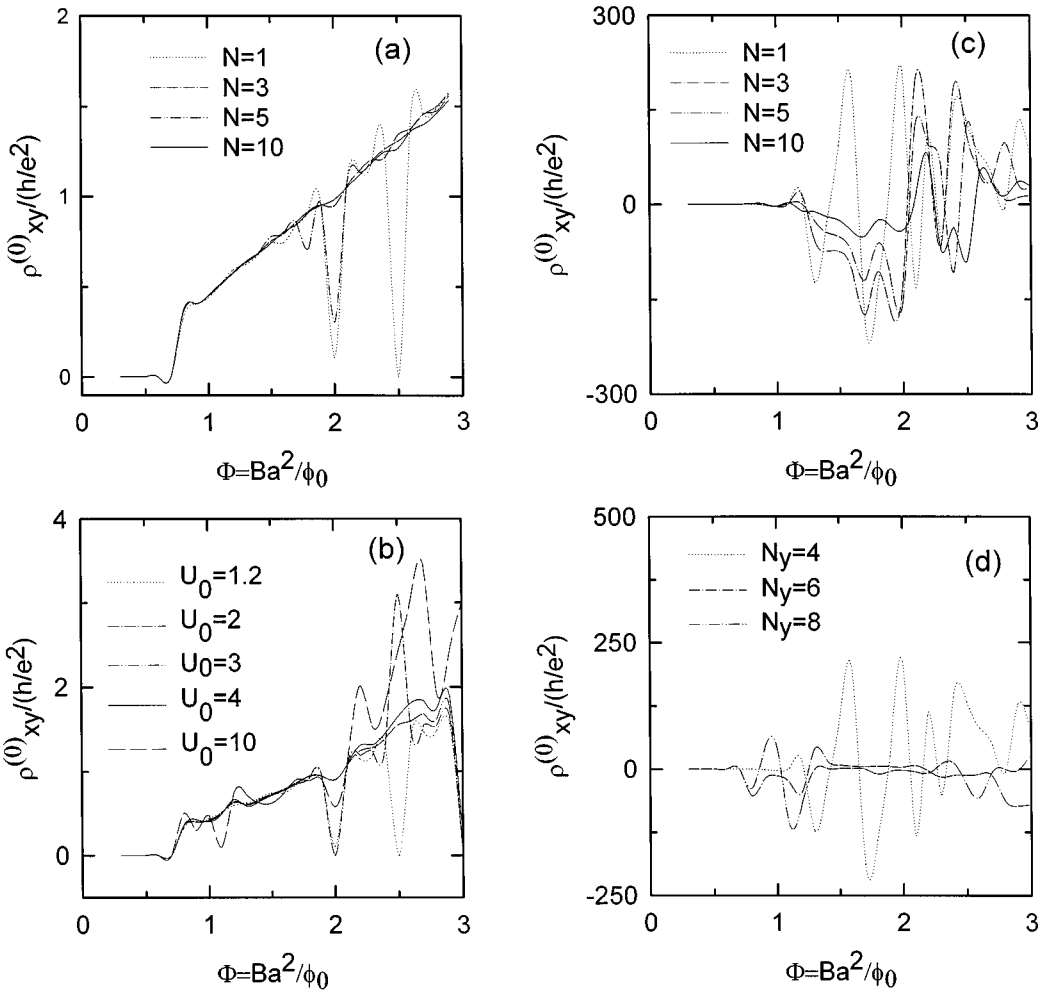

FIG. 3. Plots of ρ_{xy} as a function of the magnetic flux for the potential in Eq. (2) for (a) $U_0=1.2$ and four values of N; (b) $N=1$ and five different values of the potential strength U_0; (c) $U_0=100.0$ is fixed and N takes the values 1, 3, 5, 10; (d) $U_0=100.0$, $N=1$ for three wire lengths $L_y=N_y a$, where $a=200$ nm. The electron density is given by $n_{2D}a^2=0.5$ and the sample length in the x direction is $L_x=N_x a$, where $N_x=4$.

width of the potential barrier decreases and the QW channel becomes wider. So, the intensities of the peaks around $\Phi=1.2$ increase as N increases from one to ten in Fig. 1(d).

B. Transverse resistivity

Our results for the resistivity ρ_{xx} when the 2DEG is modulated in the x direction transverse to the direction of the channels are shown in Figs. 2(a)–2(c) for fixed N_y, i.e., wire length. In Fig. 2(a), the steepness of the slope of the potential is varied by changing the power of the cosine potential for a weak modulation $U_0=1.2$ with $L_y=80$ Å and $V_0=0.156$ meV. At low magnetic field, anomalous large peaks are obtained. These peaks are reduced when L_y is increased as shown in Fig. 2(d), where $L_y=160$ Å. These high peaks are reduced as the sample size is further increased and may even disappear completely. Therefore, we conclude that the large peak at low magnetic field is due to the finite size of the sample. Also, the high peak in Fig. 2(a) at low magnetic field is not sensitive to changes in the steepness of the potential barrier. This can be explained, as we noted in Fig. 1(a), that the Fermi level exceeds the height of the potential barrier. When $\Phi \gtrsim 1.5$, ρ_{xx} is reduced because for this range of magnetic fields the electron orbit becomes smaller than the channel width but the effect of the short length L_y is given by the slight increase in ρ_{xx} as Φ increases. The smaller the value of U_0, the more likely an electron will not be confined within a channel as it would be for large U_0 so that when the modulation potential is weak ρ_{xx} has peaks due to the nonuniform potential that an electron is subjected to. In Fig. 2(b), numerical results are presented for various strengths of the modulation potential for a fixed value of $N=1$ in the modulation potential and length $L_y=80$ Å. As U_0 varies from 1.2 (i.e., $V_0=0.156$ meV) to 10.0 (i.e., $V_0=1.265$ meV), the large peak at low magnetic field is significantly modified. When $U_0=10.0$, this large peak due to scattering off the sample boundary is altered the most. This means that when the barrier height is much larger than the Fermi energy, the model simulates short quantum wires for which ρ_{xx} has characteristics which are different from the weak modulation results at low magnetic field when the cyclotron orbits are larger than the width of the channels. As the magnetic field increases, several peaks due to scattering off the potential barriers are obtained. To support our conclusion that the large peaks in ρ_{xx} at low magnetic field are due to the bound-

ary scattering whereas the peaks at higher fields arise from the scattering off the potential barriers, we plot in Fig. 2(c) our results for a strong potential $U_0=100$ (i.e., $V_0=126.5$ meV) for several wire widths. Clearly, the effect due to the potential barrier is larger than the sample boundary since the sample boundary effect in the low-magnetic-field region is reduced and several peaks appear due to confinement by the barrier potential. Figure 2(c) shows that the heights of the peaks in ρ_{xx} decrease as N increases, i.e., as the quantum wire becomes wider the effect due to scattering off the sides is reduced. Furthermore, the peak positions are slightly changed with the QW width. We compare ρ_{xx} for various wire lengths L_y in Fig. 2(e). Giant magnetoresistance in this lateral array of wires is obtained. The peak positions depend on L_y and these calculations agree qualitatively with experimental results.[8,12]

C. Hall resistivity

Figure 3 shows our numerical results for the Hall resistivity ρ_{xy} for various potential barrier heights and steepness of the slope for the potential in Eq. (2), which complement the transverse resistivity in Fig. 2. In Figs. 3(a)–3(d), there is a quenching of ρ_{xy} at low magnetic fields. This quenching in QW's has already been explained.[9,13] As the magnetic field increases ($\Phi \gtrsim 1.0$), our calculations show that ρ_{xy} increases linearly with Φ and looks like the classical Hall effect. Actually, when $U_0=1.2$ meV, the Fermi energy is above the potential barrier and when $\Phi \gtrsim 1.0$, the cyclotron orbit is comparable with or less than the width of the QW. Consequently, the electron motion is the same as in the homogeneous 2DEG leading to the classical behavior for ρ_{xy} when $\Phi \gtrsim 1$. However, this linear increase of ρ_{xy} in the range $\Phi \gtrsim 1.0$ is modified by a strong potential barrier as shown in Fig. 3(b). The linear classical Hall effect is modified even more when U_0 is sufficiently strong, as shown in Fig. 3(c), and may disappear completely and get replaced by an anomalous Hall effect due to scattering with the wall of the QW. For a strong modulation potential, there is a negative Hall resistivity in the region of $1 \lesssim \Phi \lesssim 2$. When the width of the QW is increased (N is increased), the negative Hall resistance is reduced. Also, as seen in Fig. 3(d), when the wire length is increased, the negative Hall resistance is reduced. The negative Hall resistivity is due to the backscattering of an electron from the sample boundary when the cyclotron orbit is comparable with the length of the short QW.

IV. SUMMARY

In this paper, we calculated the transverse conductivity σ_{xx}, the longitudinal resistivity ρ_{xx}, and the Hall resistivity ρ_{xy} for a 2DEG in a perpendicular magnetic field. The modulation potential is assumed to have a simple form whose strength and steepness of slope can be varied. In the strong modulation limit, the model simulates a parallel array of quantum wires with a chosen width. We have presented numerical results for short quantum wires in the low-magnetic-field limit, i.e., $B \gtrsim 0.3$ T, using the Kubo method. The calculated results have steplike features in the transverse conductivity as the Fermi energy crosses a Landau level for weak modulation potentials and giant low-field peaks in the transverse resistivities when the potential is strong. The Hall resistivity is quenched at very low-magnetic fields. For weak modulation, our calculations show that as the magnetic field increases, ρ_{xy} increases linearly with Φ like the classical Hall effect over a range of magnetic fields when the cyclotron orbit is comparable with or less than the width of the QW so that the electron motion is the same as in the homogeneous 2DEG. This linear increase of ρ_{xy} is changed considerably by a strong potential barrier as shown in Fig. 3(b) and may disappear completely and get replaced by an anomalous Hall effect due to scattering with the wall of the QW when U_0 is sufficiently strong, as shown in Fig. 3(c). For a strong modulation potential, there is a negative Hall resistivity at higher magnetic fields, i.e., for $1<\Phi<2$. The negative Hall resistivity is reduced when the width of the QW is increased (N increases). Figure 3(d) shows that when the wire length is increased, the negative Hall resistivity is reduced. The negative Hall resistivity arises from backscattering off the edges of confinement for short quantum wires when the cyclotron orbit is comparable with the length of the short QW.

ACKNOWLEDGMENTS

The authors acknowledges the support in part from the National Science Foundation Grant No. INT-9402741 (U.S.-U.K. Collaborative Grant) and the City University of New York PSC-CUNY Grant No. 664279.

*Also at The Graduate School and University Center of the City University of New York, 33 West 42 Street, New York, NY 10036.

†Also at Toshiba Cambridge Research Center, 260 Cambridge Science Park, Milton Road, Cambridge CB4 4WE, U.K.

[1] C. Weisbuch and B. Vinter, *Quantum Semiconductor Structures* (Academic Press, New York, 1991), pp. 109–199.

[2] H. Heinrich, G. Bauer, and F. Kuchar, *Physics and Technology of Submicron Structures* (Springer, Berlin, 1988), p. 108.

[3] C. J. B. Ford *et al.*, Phys. Rev. Lett. **62**, 2724 (1989).

[4] C. J. B. Ford *et al.*, Phys. Rev. B **43**, 7339 (1988).

[5] C. J. B. Ford *et al.*, Surf. Sci. **299**, 298 (1990).

[6] G. Kirczenow and E. Castano, Phys. Rev. B **43**, 7343 (1991).

[7] M. Buttiker, Phys. Rev. B **38**, 12 724 (1988).

[8] J. E. F. Frost *et al.*, Phys. Rev. B **53**, 9602 (1996).

[9] C. J. B. Ford *et al.*, Phys. Rev. B **38**, 8518 (1988).

[10] G. Timp *et al.*, *Physics and Technology of Submicron Structures* (Springer, Berlin, 1988), p. 128.

[11] D. Huang and G. Gumbs, Phys. Rev. B **51**, 5558 (1995).

[12] G. Muller, P. Streda, D. Weiss, K. von Klitzing, and G. Weimann, Phys. Rev. B **50**, 8938 (1994).

[13] M. L. Roukes *et al.*, Phys. Rev. Lett. **59**, 3011 (1988).